

NACA TN No. 1669

3.N21/5:6/1669
1039

GOVT. DOC.

NATIONAL ADVISORY COMMITTEE FOR AERONAUTICS

TECHNICAL NOTE

No. 1669

INVESTIGATION AT LOW SPEEDS OF THE EFFECT OF ASPECT RATIO
AND SWEEP ON STATIC AND YAWING STABILITY DERIVATIVES
OF UNTAPERED WINGS

By Alex Goodman and Jack D. Brewer

Langley Aeronautical Laboratory
Langley Field, Va.



Washington
August 1948

CONN. STATE LIBRARY

AUG 23 1948

BUSINESS, SCIENCE
& TECHNOLOGY DEPT.

TECHNICAL NOTE NO. 1669

INVESTIGATION AT LOW SPEEDS OF THE EFFECT OF ASPECT RATIO
AND SWEEP ON STATIC AND YAWING STABILITY DERIVATIVES
OF UNTAPERED WINGS

By Alex Goodman and Jack D. Brewer

SUMMARY

A low-scale wind-tunnel investigation was conducted in both straight and yawing flow to determine the effects of aspect ratio and sweep (when varied independently) on the static and yawing stability derivatives for a series of untapered wings. The curved-flow equipment of the Langley stability tunnel was used for the tests.

The effects of sweep on the static stability characteristics, namely, lift-curve slope, drag, and the effective-dihedral parameter, generally became smaller as the aspect ratio decreased.

For constant sweep angle, the magnitude of the damping in yaw decreased with an increase in aspect ratio for the low lift-coefficient range. At some moderate lift coefficient, this derivative changed sign (became positive) for the 45° and 60° swept wings. For unswept wings, the experimental data indicated that the rolling moment due to yawing is very nearly proportional to the lift coefficient until maximum lift is attained. For the sweptback wings, linear variations of rolling moment due to yawing were obtained over only a limited lift range; at high lift coefficients, the values of the rolling moment due to yawing decreased and in some instances became negative near maximum lift. The rate of change of rolling moment due to yawing with lift coefficient usually increased with both sweep and aspect ratio for the low lift-coefficient range. In general, the data at low and moderate lift coefficients were in fair agreement with a simple sweep theory.

INTRODUCTION

Estimation of the dynamic flight characteristics of airplanes requires a knowledge of the component forces and moments resulting from the orientation of the airplane with respect to the air stream and from the rate of angular motion of the airplane about each of its three axes. The forces and moments resulting from the orientation of the airplane usually are expressed as the static stability derivatives, which are readily determined in conventional wind-tunnel tests. The forces and moments related to the angular motions (rotary derivatives) have generally been estimated from theory because of the lack of a convenient experimental technique.

The recent application of the rolling-flow and curved-flow principle of the Langley stability tunnel has made equally possible the determination of both rotary and static stability derivatives. Preliminary tests made in the Langley stability tunnel to investigate characteristics of swept wings indicated that, although the rotary stability derivatives of unswept wings of moderate or high aspect ratio can be predicted quite accurately from the available theory, the use of sweep - and, perhaps, low aspect ratio - introduces effects which are not readily amenable to theoretical treatment. For this reason a systematic research program has been established for the purpose of determining the effects of various geometric variables on both rotary and static stability characteristics.

The present investigation, which represents a part of the general program, is concerned with the determination of the effects of independent variations of the aspect ratio and the sweep angle on the static and yawing stability characteristics of a series of untapered wings.

SYMBOLS

The data are presented in the form of standard NACA coefficients of forces and moments, which are referred in all cases to the stability axes, with the origin at the quarter-chord point of the mean aerodynamic chord of the models tested. The positive directions of the forces, moments, and angular displacements are shown in figure 1. The coefficients and symbols used herein are defined as follows:

C_L	lift coefficient (L/qS)
C_D	drag coefficient ($-X/qS$)
C_{D_i}	induced-drag coefficient
C_Y	lateral-force coefficient (Y/qS)
C_l	rolling-moment coefficient (L'/qSb)
C_m	pitching-moment coefficient ($M/qS\bar{c}$)
C_n	yawing-moment coefficient (N/qSb)
L	lift
X	longitudinal force
Y	lateral force
L	rolling moment about X-axis

- M pitching moment about Y-axis
- N yawing moment about Z-axis
- q dynamic pressure $\left(\frac{1}{2}\rho V^2\right)$
- ρ mass density of air
- V free-stream velocity
- S wing area
- b span of wing, measured perpendicular to plane of symmetry
- c chord of wing, measured parallel to plane of symmetry
- y distance measured perpendicular to plane of symmetry
- \bar{c} mean aerodynamic chord $\left(\frac{2}{S} \int_0^{b/2} c^2 dy\right)$
- c_l chord normal to leading edge
- x distance of quarter-chord point of any chordwise section from leading edge of root section measured parallel to plane of symmetry
- \bar{x} distance from leading edge of root chord to quarter chord of mean aerodynamic chord $\left(\frac{2}{S} \int_0^{b/2} cx dy\right)$
- A aspect ratio (b^2/S)
- α angle of attack, measured in plane of symmetry
- Λ angle of sweep, degrees
- ψ angle of yaw, degrees
- $\frac{rb}{2V}$ lateral flight-path curvature (for constant sideslip, ratio of semispan to radius of curvature)
- r yawing angular velocity, radians per second

$$C_{L\alpha} = \frac{\partial C_L}{\partial \alpha}$$

$$C_{L\psi} = \frac{\partial C_L}{\partial \psi}$$

$$\bar{C}_{n_{\psi}} = \frac{\partial \bar{C}_n}{\partial \psi}$$

$$C_{Y_{\psi}} = \frac{\partial C_Y}{\partial \psi}$$

$$\bar{C}_{l_r} = \frac{\partial \bar{C}_l}{\partial \frac{rb}{2V}}$$

$$\bar{C}_{n_r} = \frac{\partial \bar{C}_n}{\partial \frac{rb}{2V}}$$

$$C_{Y_r} = \frac{\partial C_Y}{\partial \frac{rb}{2V}}$$

APPARATUS AND TESTS

The tests of the present investigation were conducted in the 6- by 6-foot curved-flow test section of the Langley stability tunnel. In this section curved flight is simulated approximately by directing the air in a curved path about a fixed model.

The models tested consisted of a series of untapered wings, all of which had NACA 0012 airfoil sections in planes normal to the leading edge. The model configurations are identified by the following designations:

Wing	Aspect ratio	Sweepback (deg)
1 2 3	1.34	0 45 60
4 5 6		0 45 60
7 8 9		0 45 60

The wing plan forms and other pertinent model data are presented in figure 2. The models were rigidly mounted on a single strut at the

quarter-chord point of the mean aerodynamic chord. (See fig. 3.) The forces and moments were measured by means of electrical strain gages mounted on the strut.

All the tests were made at a dynamic pressure of 24.9 pounds per square foot, which corresponds to a Mach number of 0.13. The sweep angles, the aspect ratios, the Reynolds numbers, and the values of $\frac{rb}{2V}$ corresponding to the four air-stream curvatures used are presented in table I. The first Reynolds number given is, as is customary, based on the mean aerodynamic chord and the free-stream velocity. Some evidence is available to indicate that a Reynolds number based on the chord and velocity normal to the leading edge is of greater significance than the conventional Reynolds number with regard to separation phenomena. (See reference 1.) For this reason the second Reynolds number has been included in the table.

The aerodynamic characteristics of the wings were determined in both straight and yawing flow. In the straight-flow tests six-component measurements were obtained for each wing through an angle-of-attack range from approximately zero lift up to and beyond maximum lift at angles of yaw of 0° and $\pm 5^\circ$. The yawing-flow tests were made for zero yaw angle and at four different wall curvatures corresponding to the values of $\frac{rb}{2V}$ shown in table I. Each model was tested in yawing flow through an angle-of-attack range from approximately zero lift up to and beyond maximum lift.

CORRECTIONS

The following corrections for jet-boundary effects were applied to the data:

$$\Delta C_L = KC_{L_T}$$

$$\Delta \alpha = 57.3 \delta_w \frac{S}{C} C_L$$

$$\Delta C_D = \delta_w \frac{S}{C} C_L^2$$

where

- δ_w boundary-correction factor obtained from reference 2
- C tunnel cross-sectional area
- C_{L_T} uncorrected tunnel rolling-moment coefficient
- K correction factor from reference 3 modified for application to present tests

The lateral-force coefficient has been corrected for the buoyancy effect of the static-pressure gradient associated with curved flow, according to the following equation:

$$\Delta C_Y = 4.0 \frac{v}{bS} \frac{rb}{2V}$$

where v is the volume of the model.

An approximate angle-of-attack correction for deflections resulting from the aerodynamic loads has been applied to the data of the present investigation.

The values of C_{l_r} have been corrected for the tare associated with the induced load resulting from the presence of the strut with the wing at zero angle of attack. The same correction was applied throughout the angle-of-attack range. No other tare corrections have been applied to the data. No corrections have been applied for the effects of blocking or for any effects of turbulence or static-pressure gradient on the boundary-layer flow.

RESULTS AND DISCUSSION

Presentation of Data

The static stability characteristics of the present series of wings are given in figures 4 to 9. Results of the tests made through the angle-of-attack range for $\pm 5^\circ$ yaw are not presented because they were used only for determining the lateral stability derivatives presented in figures 8 and 9. The basic yawing-flow data for a part of the present series of wings are presented in figure 10. The yawing stability characteristics are presented in figures 11 to 14.

Characteristics in Straight Flow

Lift. - In general, the maximum lift coefficient obtained for the wings tested increased with sweep for constant aspect ratio (fig. 4). Since the tests were made at low Reynolds numbers (see table I), very little significance can be attributed to this result. Past experience has shown that the maximum lift coefficient for an unswept wing decreases as the scale of the test decreases. Comparison of results from large-scale tests of tapered wings made in the Ames 40- by 80-foot wind tunnel with low-scale test results indicates that, while such a decrease can be quite large for unswept wings, it may be relatively small for highly swept wings.

An application of simple sweep theory given in reference 4 indicates that $C_{L\alpha}$ may be expressed by the following relation:

$$(C_{L\alpha})_{\Lambda} = \frac{(A + 2) \cos \Lambda}{A + 2 \cos \Lambda} (C_{L\alpha})_{\Lambda=0^\circ}$$

The variation of $C_{L\alpha}$ with sweep angle determined from these tests is compared in figure 5 with the values of $C_{L\alpha}$ obtained from the aforementioned relation and by the theory of Weissinger (reference 5). A section lift-curve slope of 0.105 was used for the Weissinger computations because it was considered appropriate for the conditions of the present tests. In general, the two theoretical methods yield approximately the same results, although the Weissinger method is in better agreement with experiment at low aspect ratios and the simple theory is in better agreement with the results at the high aspect ratios. Both theories are in qualitative agreement with experiment in that they show that the effect of sweep becomes smaller as the aspect ratio decreases.

Drag.- Theoretical calculations (reference 6) have shown the relation

$$C_{D_i} = \frac{C_L^2}{\pi A}$$

for the induced drag of unswept elliptic wings to be approximately correct for the induced drag of swept wings also. Curves of $C_L^2/\pi A$ are included in figure 4 for comparison with the experimental drag curves. The difference ΔC_D between the total drag and the induced drag represents that part of the drag not ideally associated with the lift. For some of the wings (particularly the low-aspect-ratio wings 1, 2, and 4), the increment ΔC_D decreases with an increase of lift coefficient, and at the same time the lift-curve slope increases. This effect probably results from a reduction in the ability of the trailing vortices to produce downwash in the plane of the wing as the angle of attack increases. Tests (reference 7) of other low-aspect-ratio wings gave similar results. The high drag coefficients (particularly at low lift coefficients) obtained for wings 8 and 9 probably can be attributed to the drag of the steel model support bracket used for mounting these wings in the tunnel. (See fig. 3(b).) The increment ΔC_D generally was considerably larger at high lift coefficients for swept wings than for unswept wings. The effect of sweep on ΔC_D became smaller, however, as the aspect ratio decreased.

Longitudinal stability.- The effects of aspect ratio and sweep on the longitudinal stability at high lift coefficients for the wings of the present tests are in good agreement with the results of reference 8. The region indicating the boundary between satisfactory and unsatisfactory longitudinal stability at high lift coefficients, obtained from figure 41 of reference 8, is reproduced in figure 6 of the present paper.

The positions in figure 6 of wings 6, 8, and 9 indicate unfavorable longitudinal stability at high lift coefficients, which is shown by the pitching-moment curves of figure 4. Figure 4 indicates that wings 3 and 5, although in the boundary region in figure 6, and the remaining wings, located in the stable region in figure 6, have favorable longitudinal stability characteristics at high lift coefficients.

The effect of both aspect ratio and sweep on the aerodynamic-center location is shown in figure 7 to be small for the untapered wings of the present investigation.

Lateral and directional stability.- The slope $\left(\frac{\partial C_{l_{\psi}}}{\partial C_L}\right)$ obtained from figure 8 is plotted against sweep angle in figure 9 and compared with values of $\left(\frac{\partial C_{l_{\psi}}}{\partial C_L}\right)$ obtained from the relation

$$\left(\frac{\partial C_{l_{\psi}}}{\partial C_L}\right)_{\Lambda} = \left(\frac{\partial C_{l_{\psi}}}{\partial C_L}\right)_{\Lambda=0^{\circ}} + \frac{1}{4} \frac{\tan \Lambda}{57.3} \left(\frac{A + 2 \cos \Lambda}{A + 4 \cos \Lambda}\right)$$

from reference 4. The experimental values of $\left(\frac{\partial C_{l_{\psi}}}{\partial C_L}\right)_{\Lambda=0^{\circ}}$ were used in the foregoing expression to arrive at the calculated values for the swept wings. The agreement in most cases is good, although the theoretical values appear to underestimate the effects of sweep. At some moderate lift coefficient the variation of $C_{l_{\psi}}$ with C_L became nonlinear. The lift coefficient at which this condition occurred decreased with sweep. As in the case of $C_{L_{\alpha}}$, the effects of sweep on $C_{l_{\psi}}$ became smaller as the aspect ratio decreased.

The derivatives $C_{n_{\psi}}$ and $C_{y_{\psi}}$ are generally erratic. (See fig. 8.) It should be noted that $C_{n_{\psi}}$ was almost always negative (indicating positive stability) at low and moderate lift coefficients but became positive before maximum lift was reached. It appears that the instability of the wing alone near maximum lift may be large enough, in some cases, to overbalance the stabilizing effect of the vertical tail for the complete airplane.

Characteristics in Yawing Flow

Damping in yaw.- Theoretical values of C_{n_r} obtained from reference 4 are compared with the experimental results in figure 11. The effects of profile drag have been included in these theoretical values. In general,

the theoretical and experimental variations of C_{nr} with C_L agree very well over a moderate range of lift coefficient. For constant sweep angle, C_{nr} decreased with an increase in aspect ratio for the low lift-coefficient range. At some moderate lift coefficient, the damping in yaw changes sign and becomes positive for wings 3, 5, 6, 8, and 9. The lift coefficient at which this change occurs tends to decrease with an increase in aspect ratio and sweep.

Rolling moment due to yawing.- Experimental and theoretical values of the rolling moment due to yawing C_{lr} plotted against lift coefficient are compared in figure 12. In general, the theory appears to underestimate the effects of sweep on this derivative. For unswept wings (wings 1, 4, and 7), the experimental data indicate that C_{lr} is very nearly proportional to the lift coefficient until maximum lift is attained. For the sweptback wings, linear variations are obtained over only a limited lift range; at high lift coefficients, the values of C_{lr} decrease and, in some instances, become negative near maximum lift.

Comparisons of the experimental and theoretical values of the slope $\partial C_{lr}/\partial C_L$, taken at low lift coefficients, are presented in figure 13. The trends resulting from sweep and aspect ratio appear to be properly predicted by the theory, although the magnitude of the effect of sweep is considerably underestimated. In general, the slope $\partial C_{lr}/\partial C_L$ increases with both sweep and aspect ratio.

Lateral force due to yawing.- In figure 14, the variation of the experimental and theoretical values (reference 4) of C_{Yr} with lift coefficient is presented. This derivative is probably of very little significance.

CONCLUSIONS

The results of low-scale tests made in both straight and yawing flow on a series of untapered wings to determine the effects of aspect ratio and sweep (when varied independently) on the static and yawing derivatives (for zero sideslip) indicate the following conclusions:

1. In general, the effects of sweep on the static stability characteristics, namely, lift-curve slope, drag, and the effective-dihedral parameter, became smaller as the aspect ratio decreased.

2. For constant sweep angle, the magnitude of the damping in yaw decreased with an increase in aspect ratio for the low lift-coefficient range. At some moderate lift coefficient, this derivative changed sign (became positive) for 45° and 60° swept wings.

3. For unswept wings, the experimental data indicate that the rolling moment due to yawing is very nearly proportional to the lift coefficient until maximum lift is attained. For the sweptback wings, linear variations were obtained over only a limited lift range; at high lift coefficients, the values of the rolling moment due to yawing decreased and, in some instances, became negative near maximum lift. The rate of change of rolling moment due to yawing with lift coefficient usually increased with both sweep and aspect ratio for the low lift-coefficient range.

4. In general, the data at low and moderate lift coefficients were in fair agreement with a simple sweep theory.

Langley Aeronautical Laboratory
National Advisory Committee for Aeronautics
Langley Field, Va., March 29, 1948

REFERENCES

1. Jones, Robert T.: Effects of Sweepback on Boundary Layer and Separation. NACA TN No. 1402, 1947.
2. Silverstein, Abe, and White, James A.: Wind-Tunnel Interference with Particular Reference to Off-Center Positions of the Wing and to the Downwash at the Tail. NACA Rep. No. 547, 1935.
3. Swanson, Robert S.: Jet-Boundary Corrections to a Yawed Model in a Closed Rectangular Wind Tunnel. NACA ARR, Feb. 1943.
4. Toll, Thomas A., and Queijo, M. J.: Approximate Relations and Charts for Low-Speed Stability Derivatives of Swept Wings. NACA TN No. 1581, 1948.
5. Weissinger, J.: The Lift Distribution of Swept-Back Wings. NACA TM No. 1120, 1947.
6. Mutterperl, William: The Calculation of Span Load Distributions on Swept-Back Wings. NACA TN No. 834, 1941.
7. Zimmerman, C. H.: Characteristics of Clark Y Airfoils of Small Aspect Ratios. NACA Rep. No. 431, 1932.
8. Shortal, Joseph A., and Maggin, Bernard: Effect of Sweepback and Aspect Ratio on Longitudinal Stability Characteristics of Wings at Low Speeds. NACA TN No. 1093, 1946.

TABLE I.- TEST CONDITIONS AND CONFIGURATIONS

Sweep angle (deg)	Aspect ratio.	Reynolds number based on \bar{c} and V	Reynolds number based on c_l and $V \cos \Lambda$	Lateral flight-path curvature, $\frac{rb}{2V}$
0	1.34	1,580,000	1,580,000	0, -0.0229, -0.0486, -0.0640
	2.61	1,100,000	1,100,000	0, -0.0319, -0.0677, -0.0891
	5.16	780,000	780,000	0, -0.0442, -0.0937, -0.1234
45	1.34	1,560,000	780,000	0, -0.0229, -0.0485, -0.0638
	2.61	1,100,000	550,000	0, -0.0316, -0.0670, -0.0883
	5.16	770,000	385,000	0, -0.0442, -0.0937, -0.1234
60	1.34	1,560,000	390,000	0, -0.0229, -0.0485, -0.0639
	2.61	1,080,000	270,000	0, -0.0316, -0.0670, -0.0882
	5.16	760,000	190,000	0, -0.0444, -0.0942, -0.1241



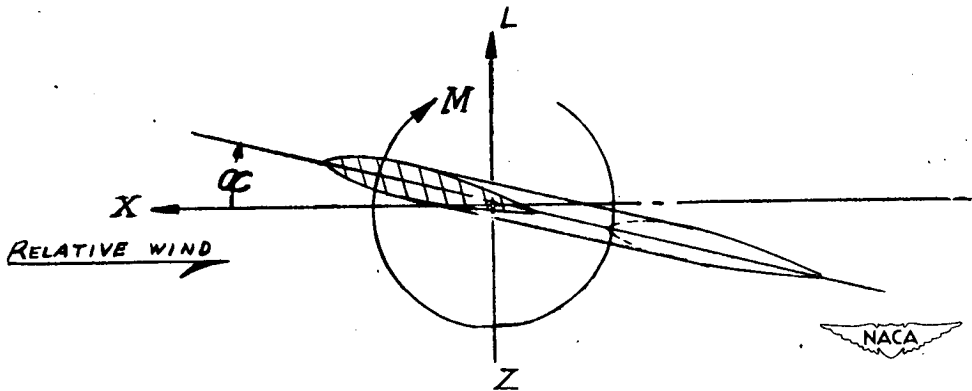
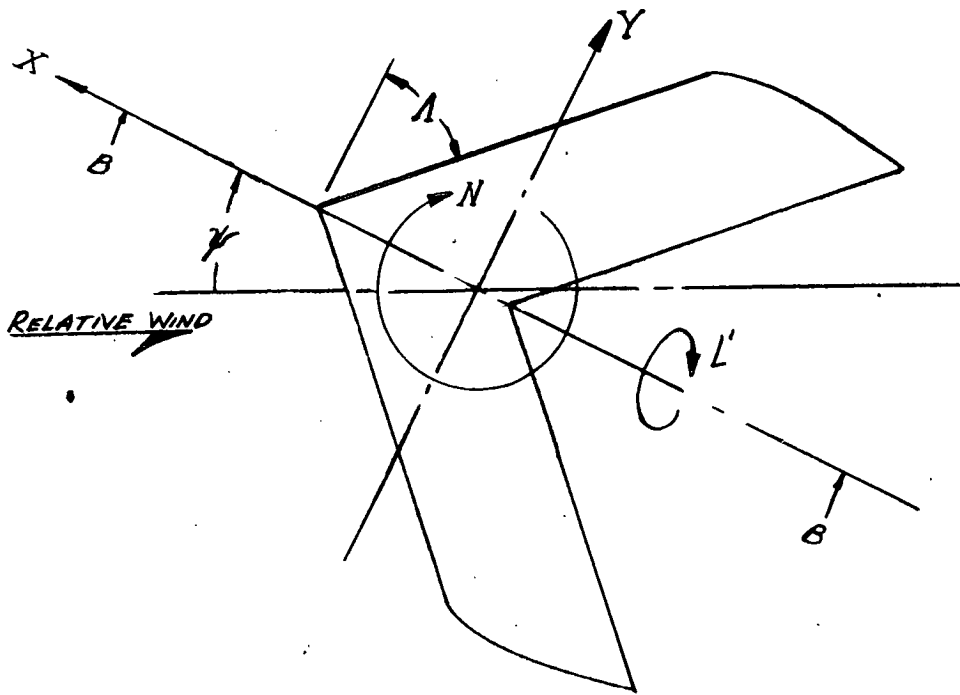


Figure 1.- System of axes used. Positive directions of forces, moments, and angles are indicated.

Λ (deg)	Wing	A	S (sq ft)	b (ft)	\bar{c} (ft)	\bar{x} (ft)
0	1	1.34	3.04	2.21	1.68	.41
	4	2.61	3.60	3.08	1.18	.30
	7	5.16	3.52	4.26	.83	.21

45	2	1.34	3.62	2.20	1.66	.96
	5	2.61	3.56	3.05	1.17	1.05
	8	5.16	3.50	4.26	.83	1.26

60	3	1.34	3.64	2.21	1.65	1.36
	6	2.61	3.53	3.05	1.16	1.60
	9	5.16	3.56	4.28	.83	2.06

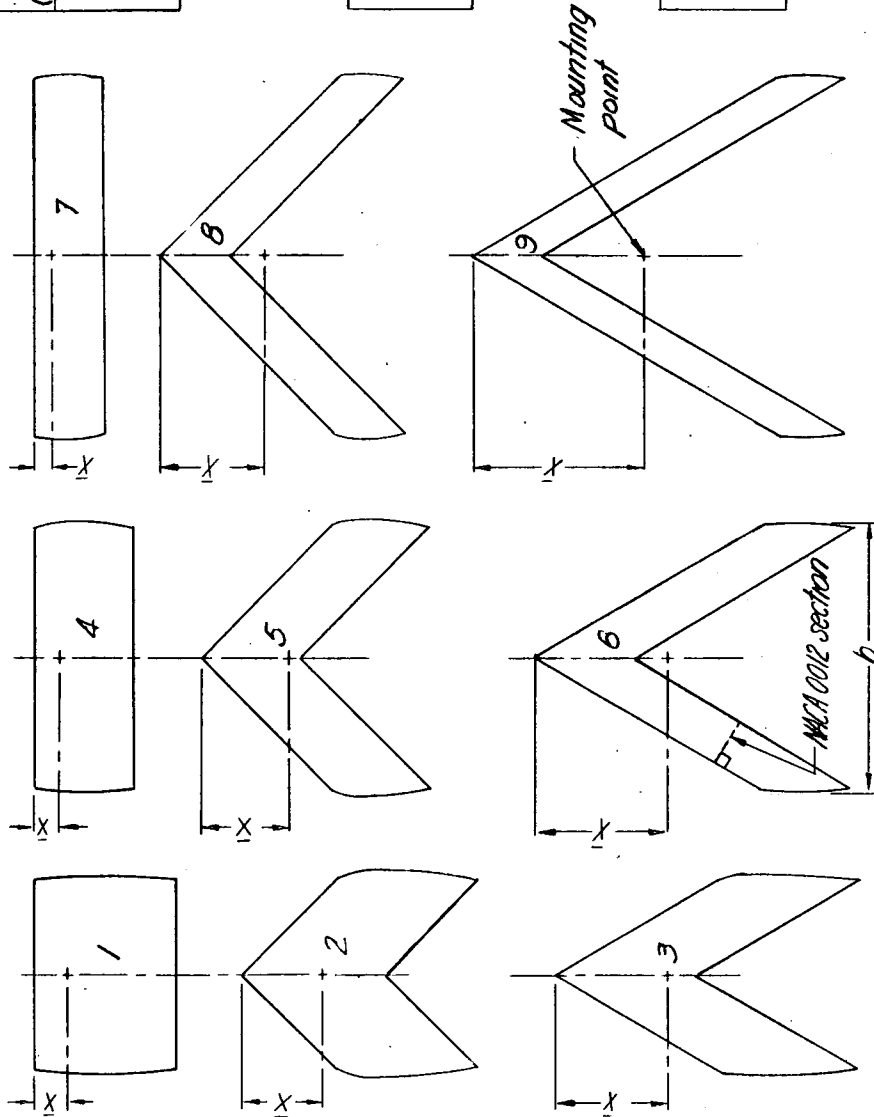
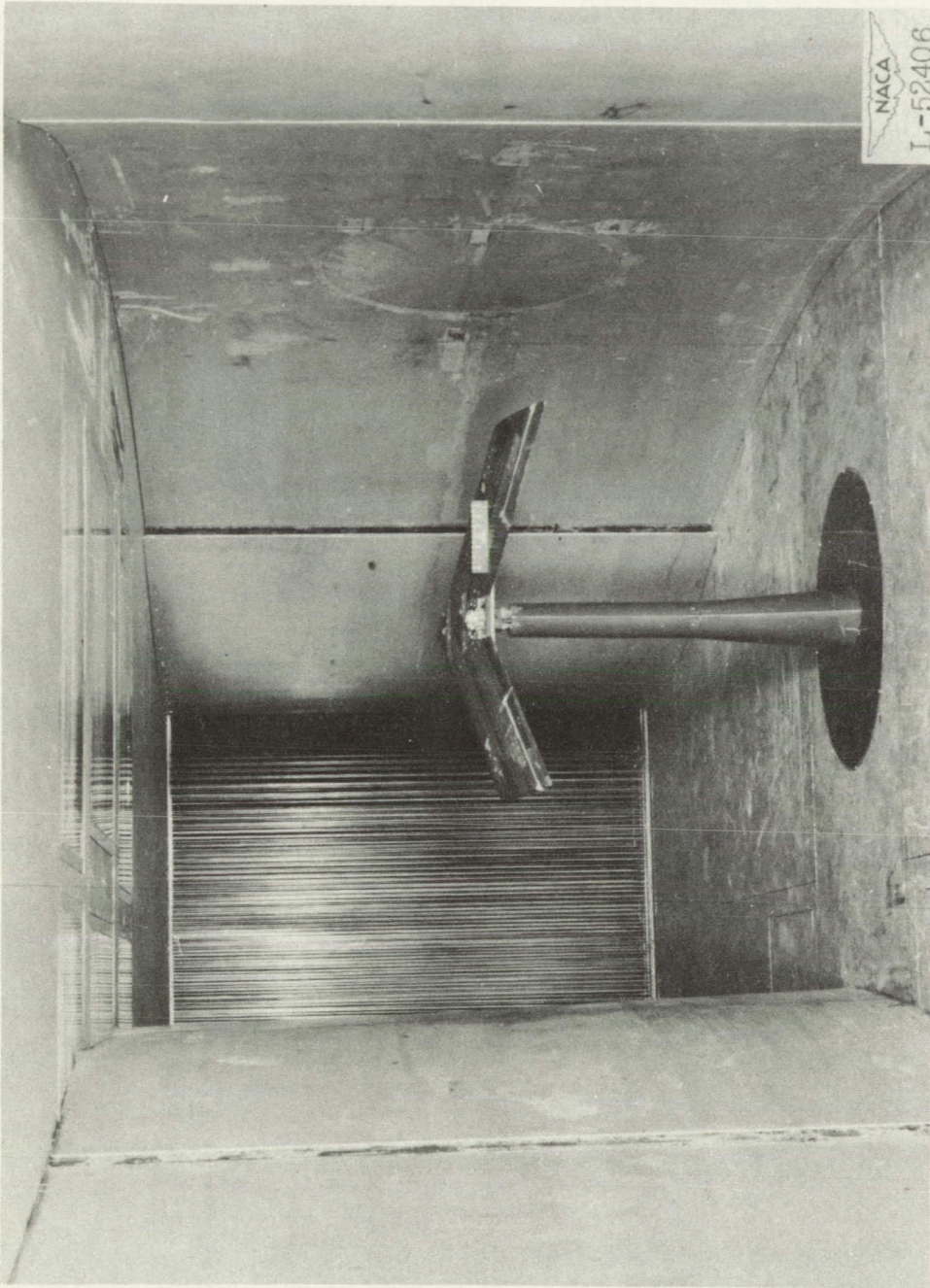


Figure 2. - Plan forms of sweptback wings; NACA 0012 profile (perpendicular to leading edge).

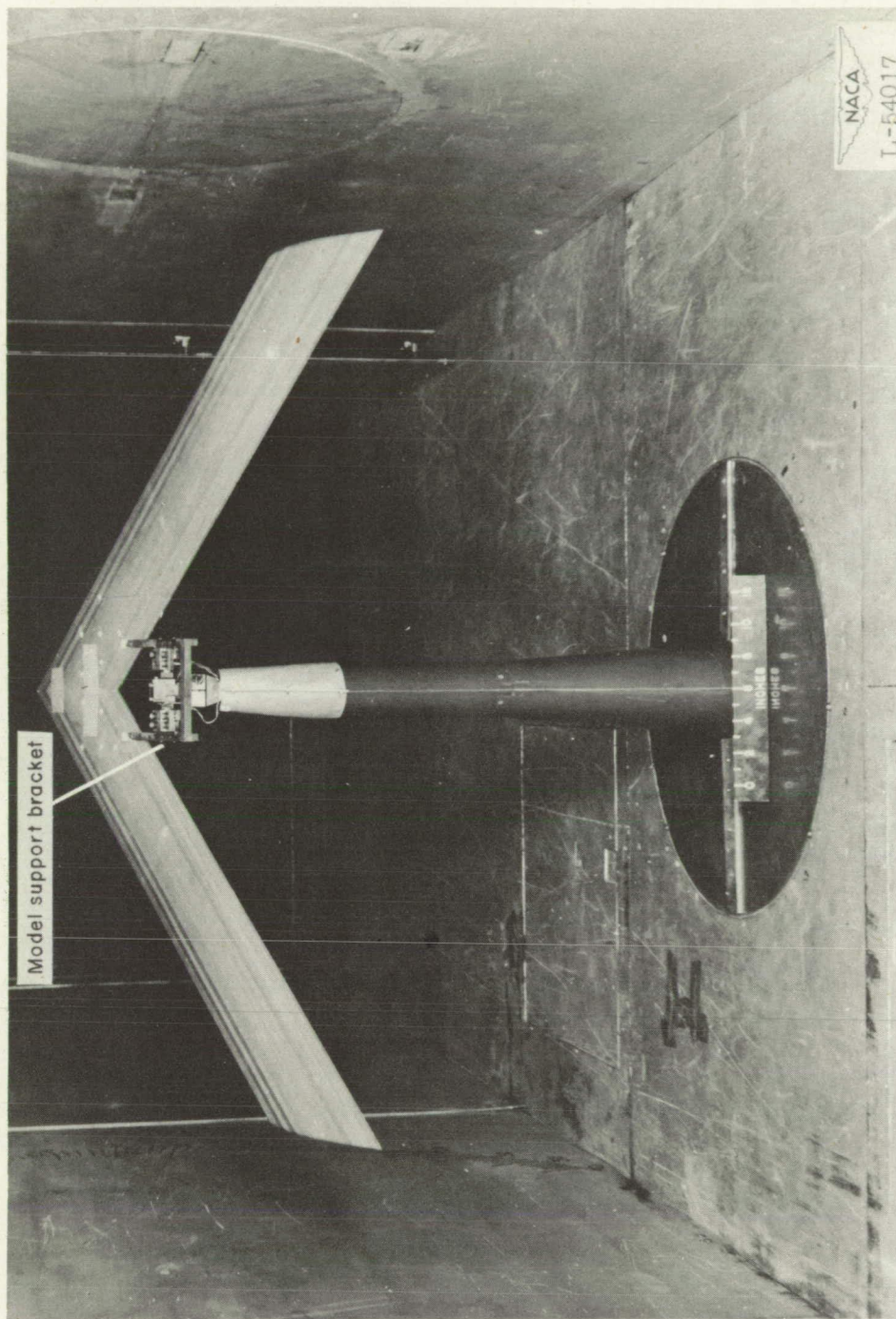


(a) Wing 5; $A = 2.61$; $\Lambda = 45^\circ$.

Figure 3.- Wings mounted in curved-flow test section of the Langley stability tunnel.

Page intentionally left blank

Page intentionally left blank



(b) Wing 8; $A = 5.16$; $\Lambda = 45^\circ$.

Figure 3.- Concluded.

Page intentionally left blank

Page intentionally left blank

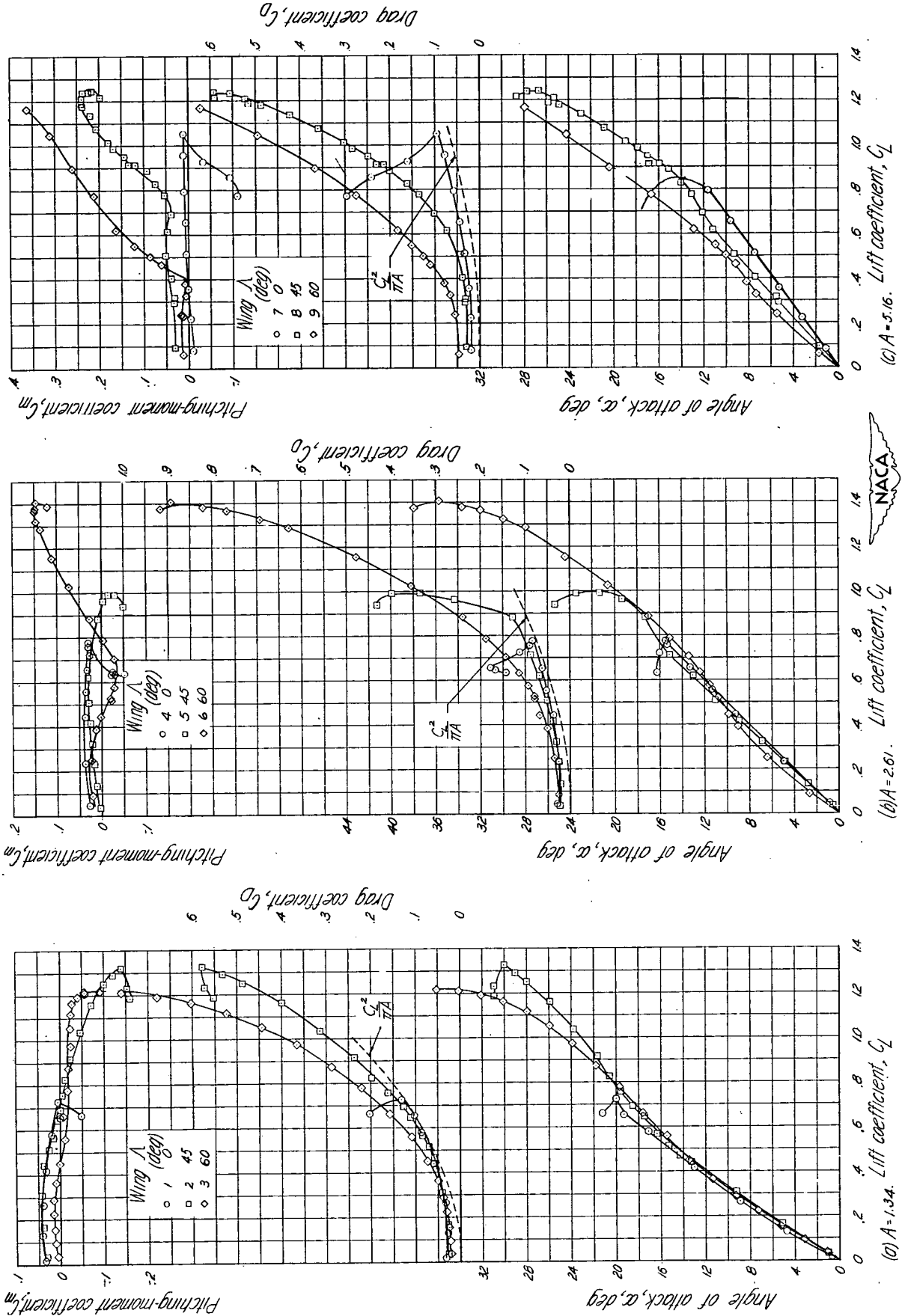


Figure 4.- Variation with lift coefficient of the aerodynamic characteristics of a series of swept wings.

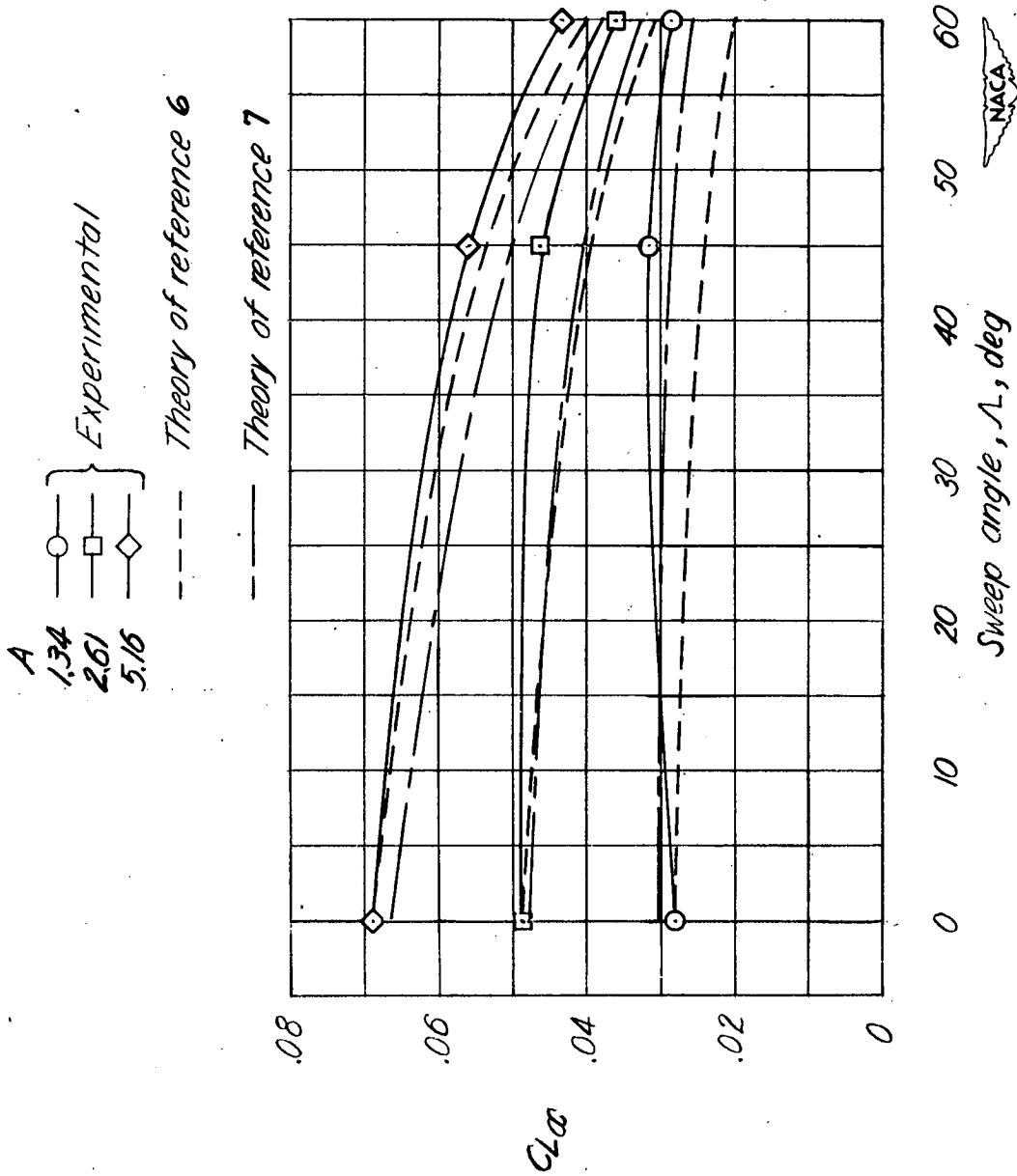

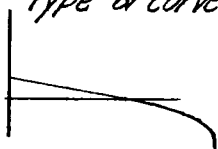

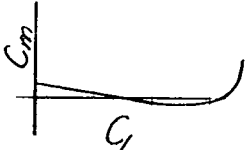


Figure 5- Variation with sweep angle of the experimental and theoretical values of lift-curve slope.

Rating	Symbol	Type of curve of C_m against C_L at high C_L
Stable		
Unstable		

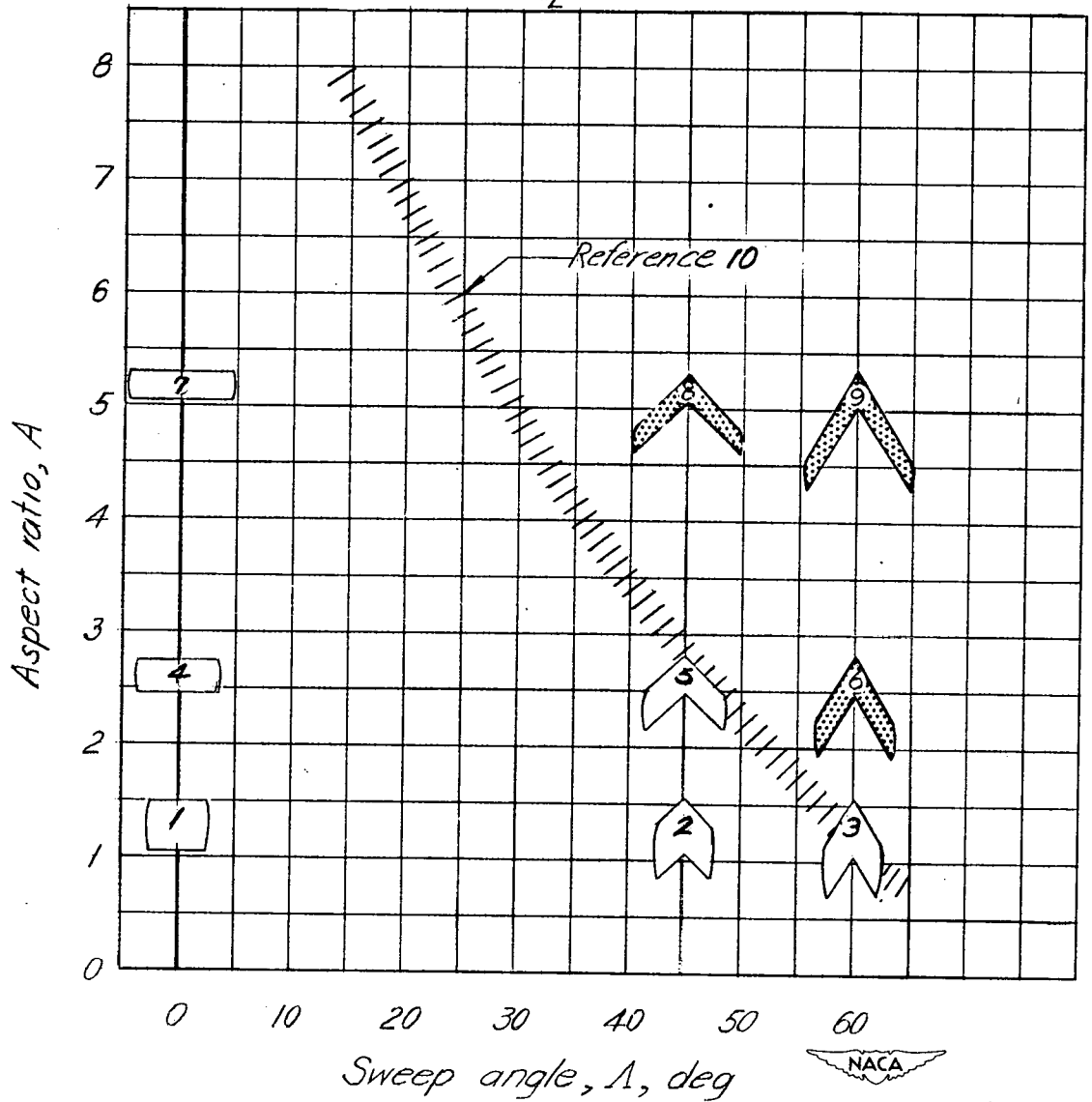


Figure 6.- Chart summarizing the effects of aspect ratio on the pitching-moment curve of swept-back wings at high lift coefficients.

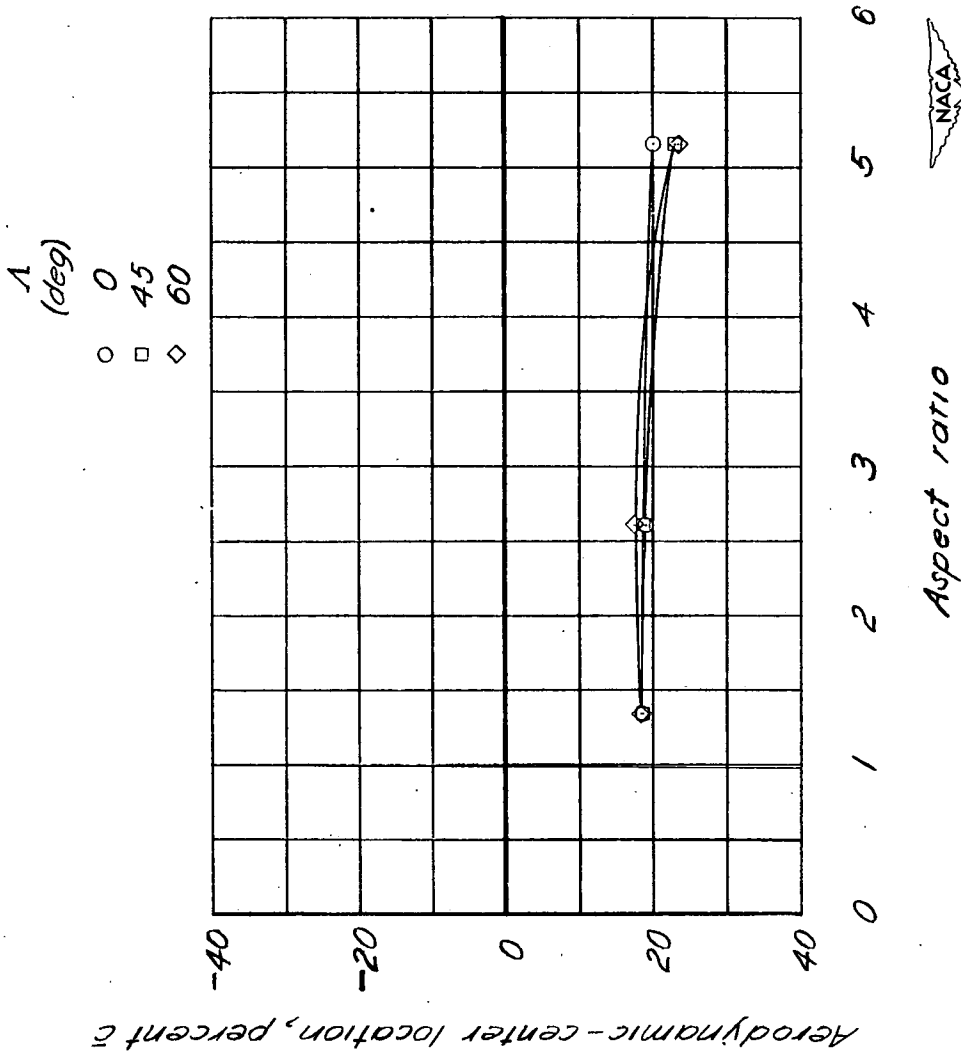


Figure 7. - Effects of aspect ratio and sweep on the aerodynamic-center location. $C_L = 0$.

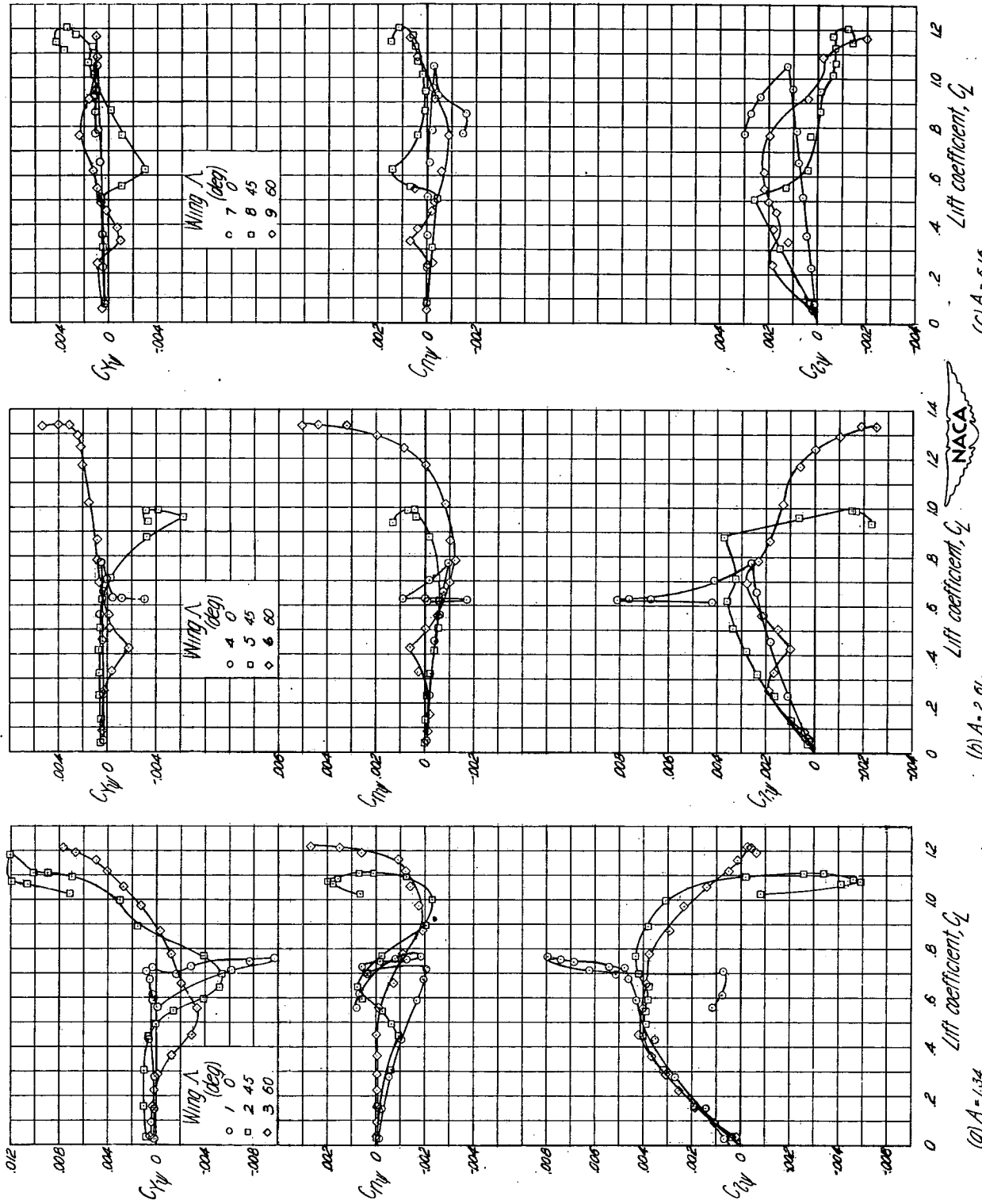
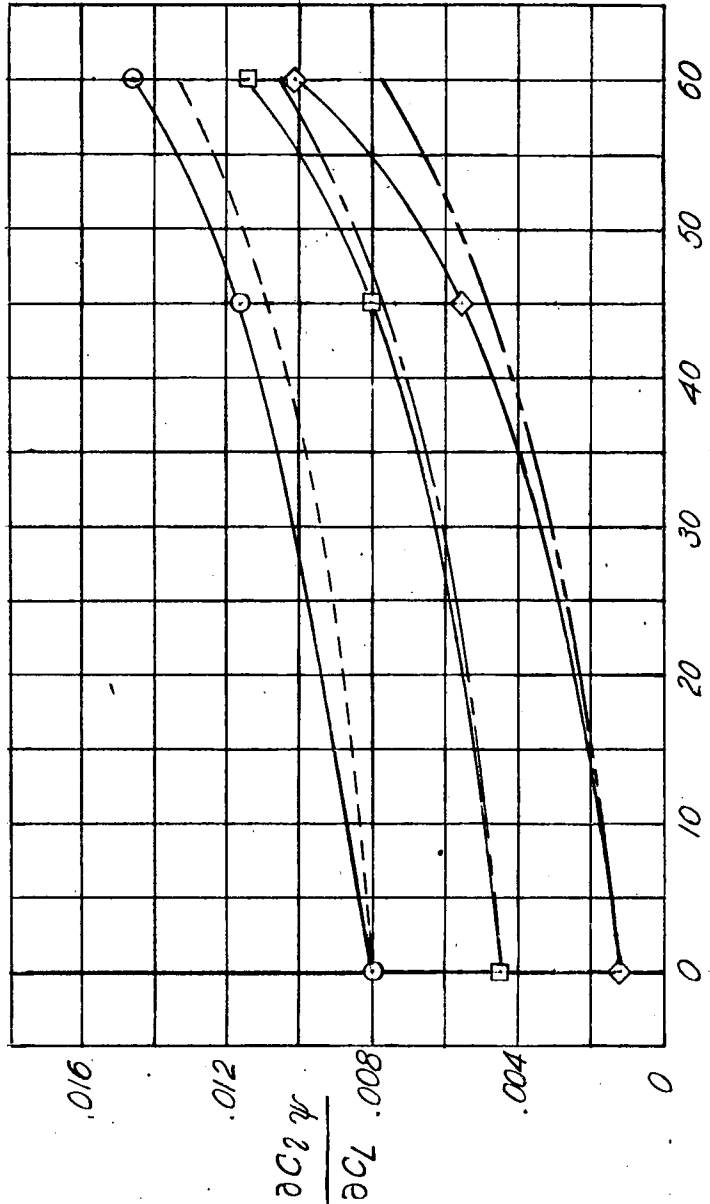


Figure 8 - Variation of C_{xy} , C_{ny} , and C_{py} with lift coefficient.

A Experimental Theory of reference 6

1.34 —○—
 2.61 —□—
 5.16 —◇—



Sweep angle, Λ , deg

Figure 9. - Variation with sweep angle of the experimental and theoretical values of $\frac{\partial C_L}{\partial \Lambda}$.

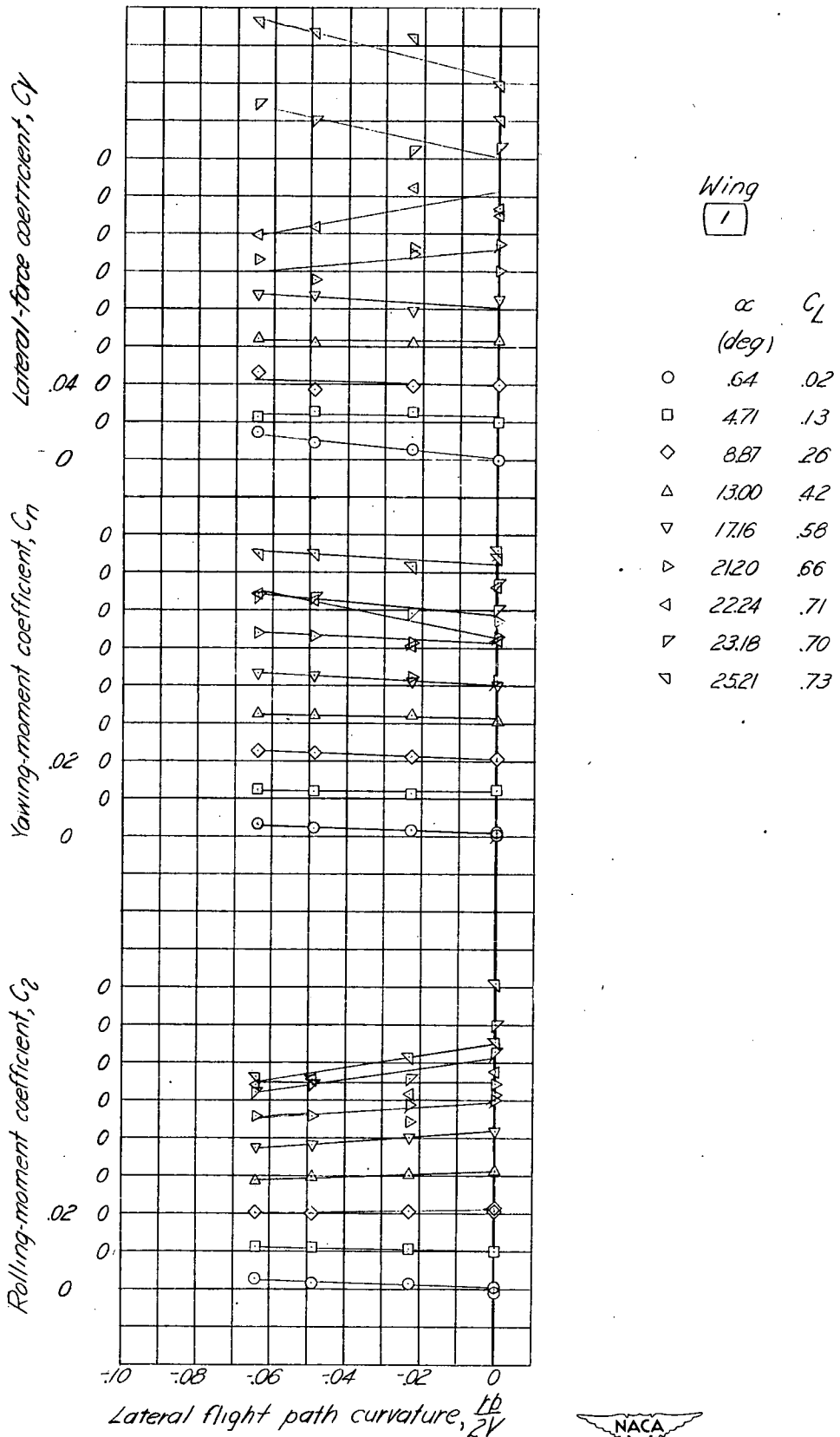


Figure 10.- Variation with lateral flight-path curvature of the lateral characteristics for a series of swept wings.

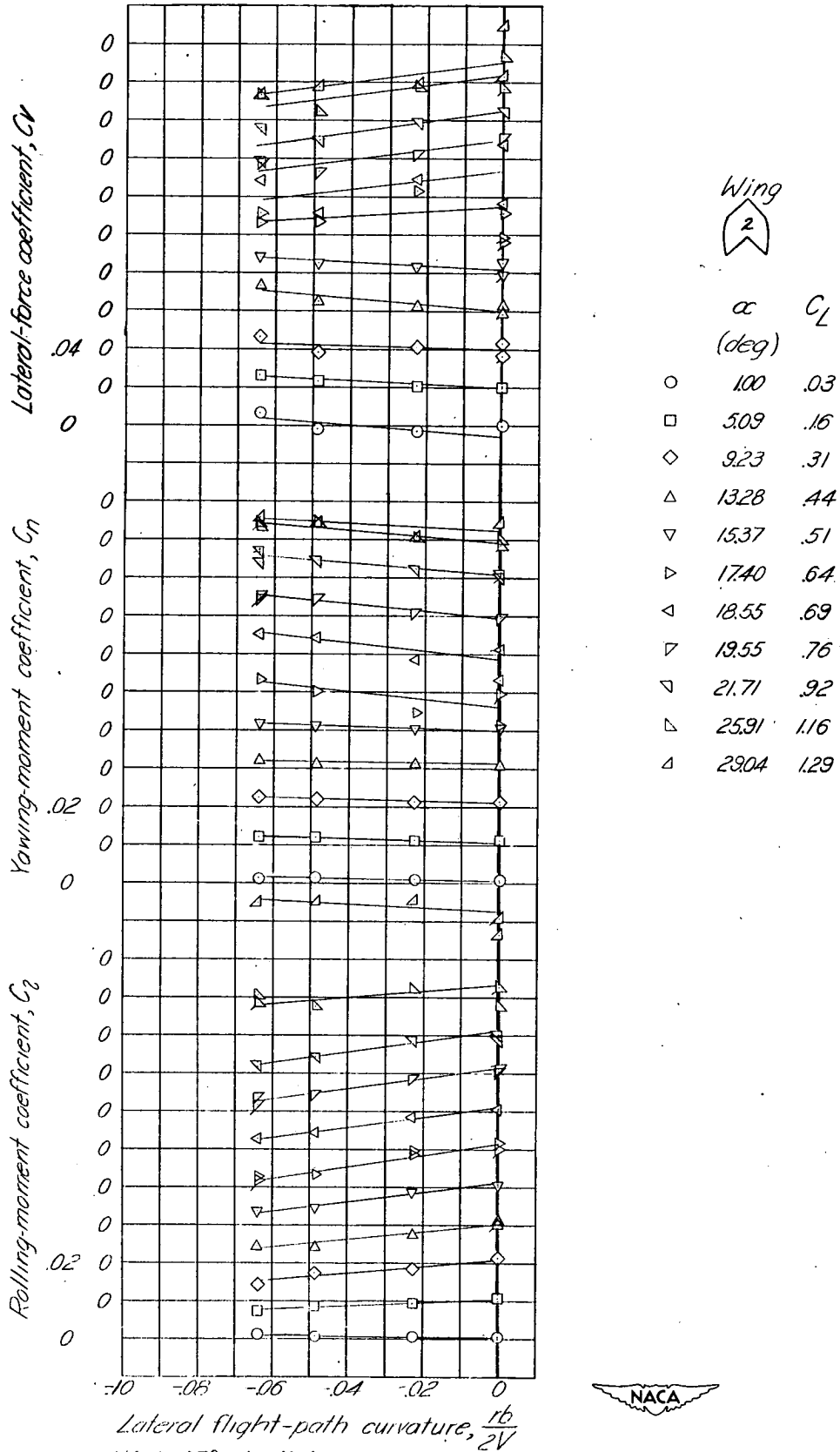


Figure 10.-Continued.



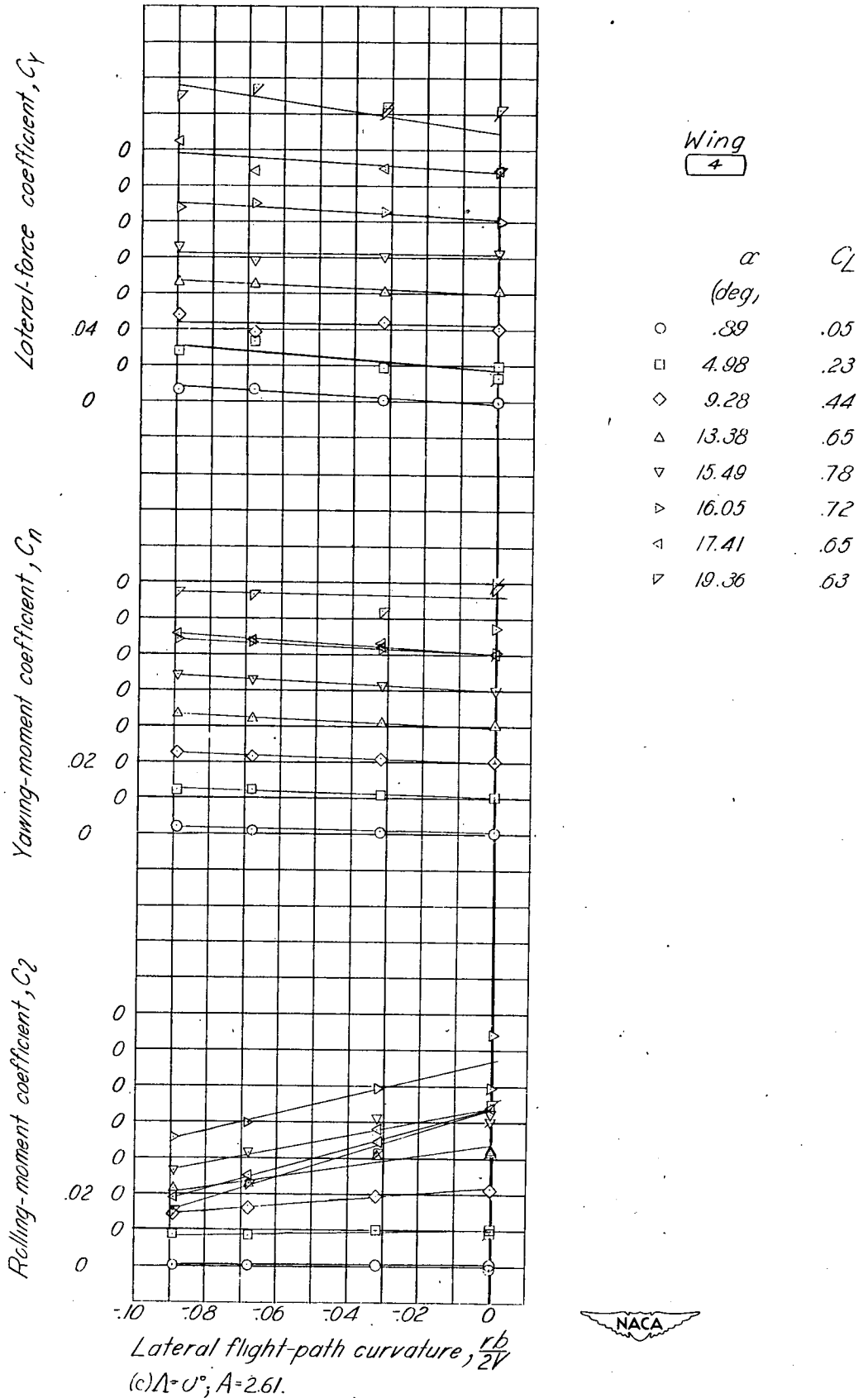
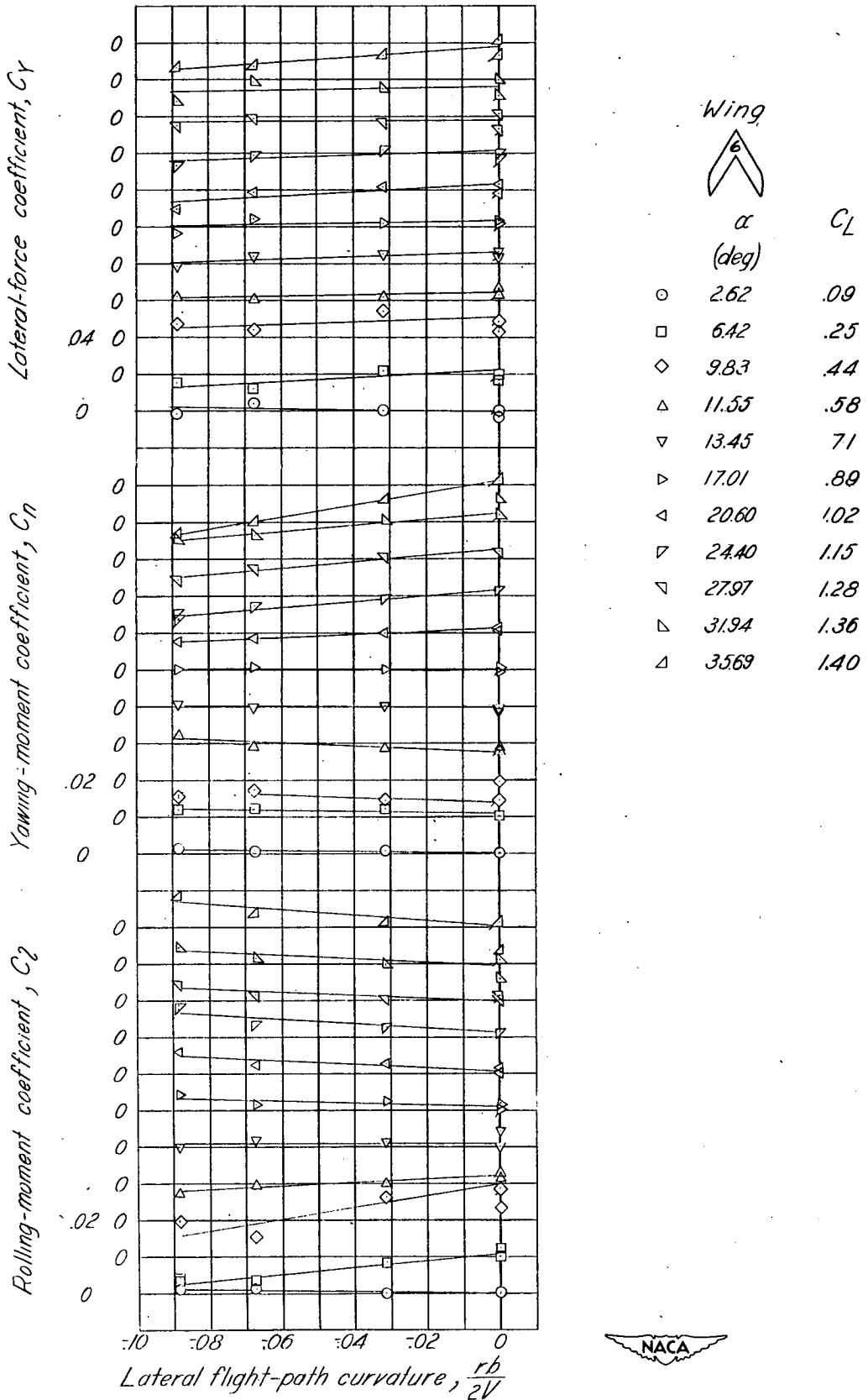


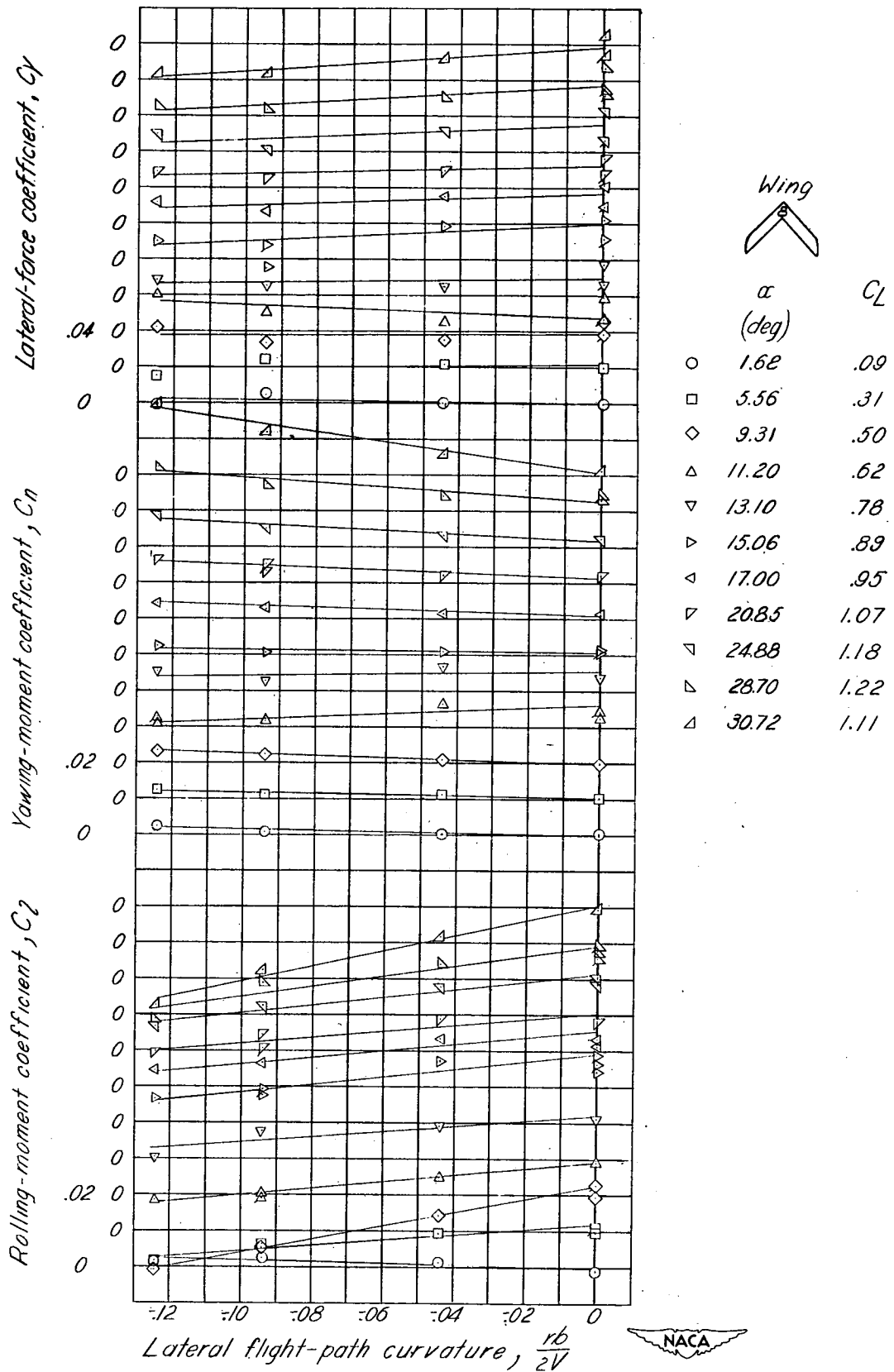
Figure 10. Continued.



(d) $\Lambda = 60^\circ$; $A = 2.61$.

Figure 10. Continued.

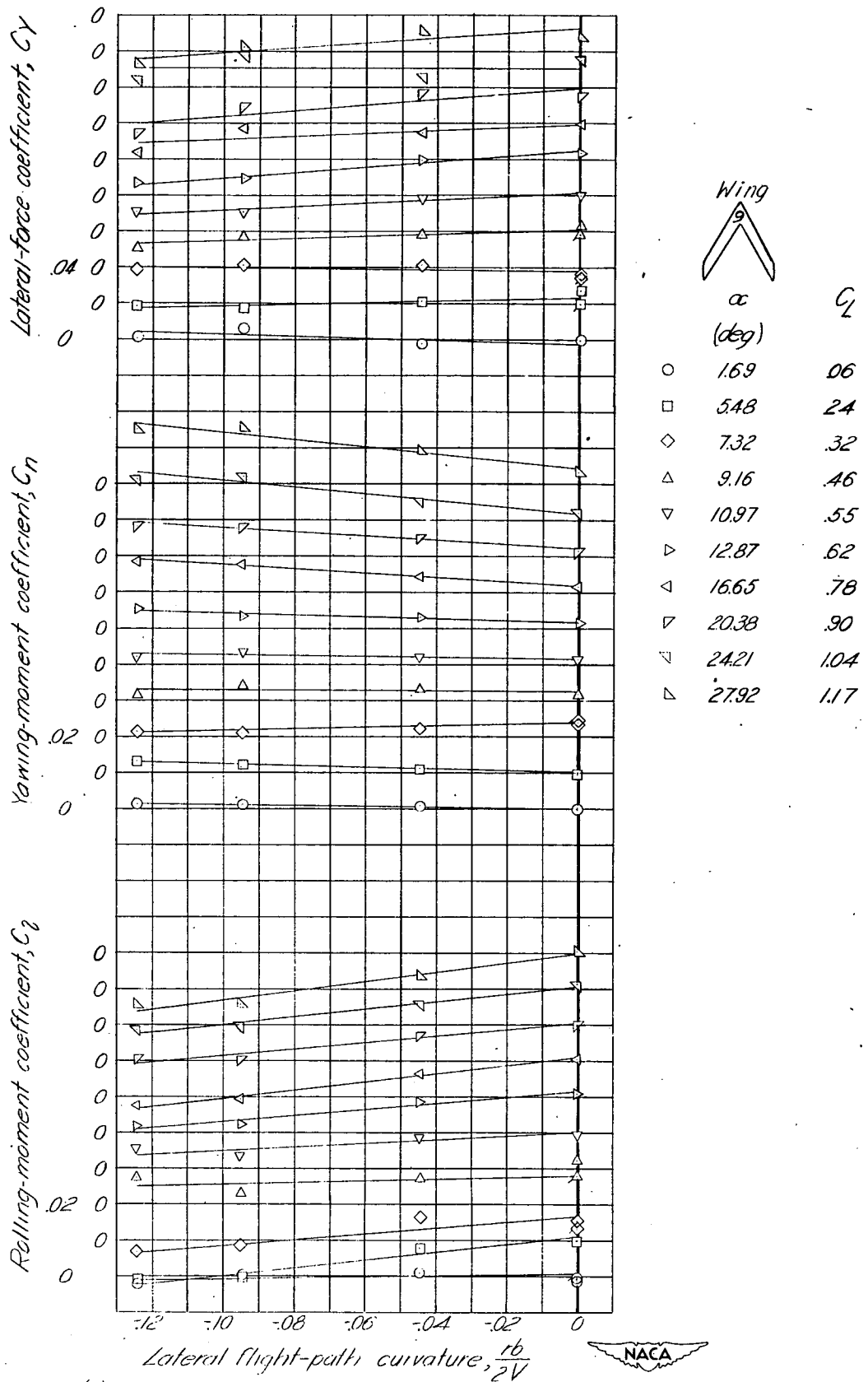




(e) $\Lambda = 45^\circ$; $A = 5.16$

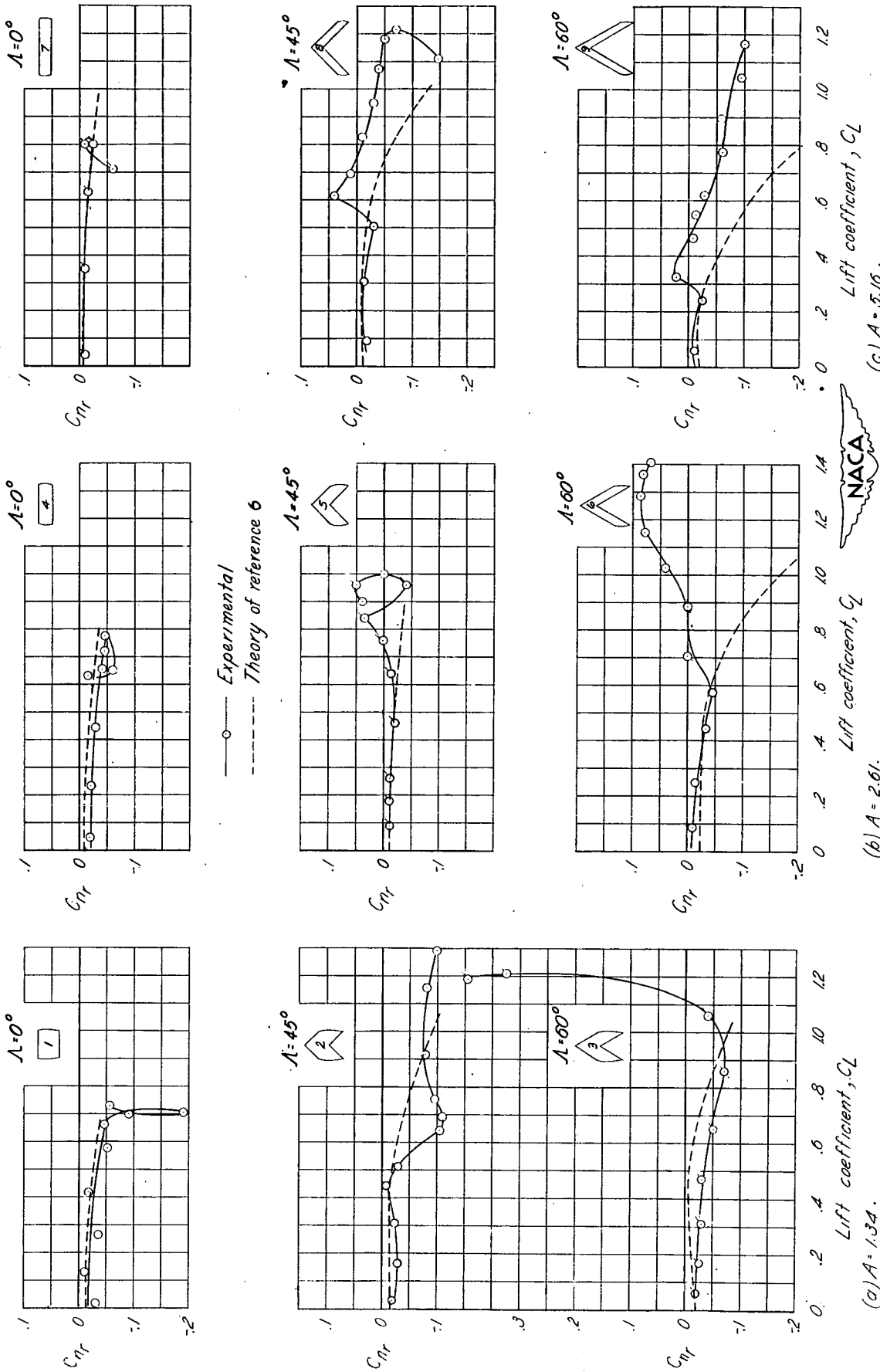
Figure 10.- Continued.





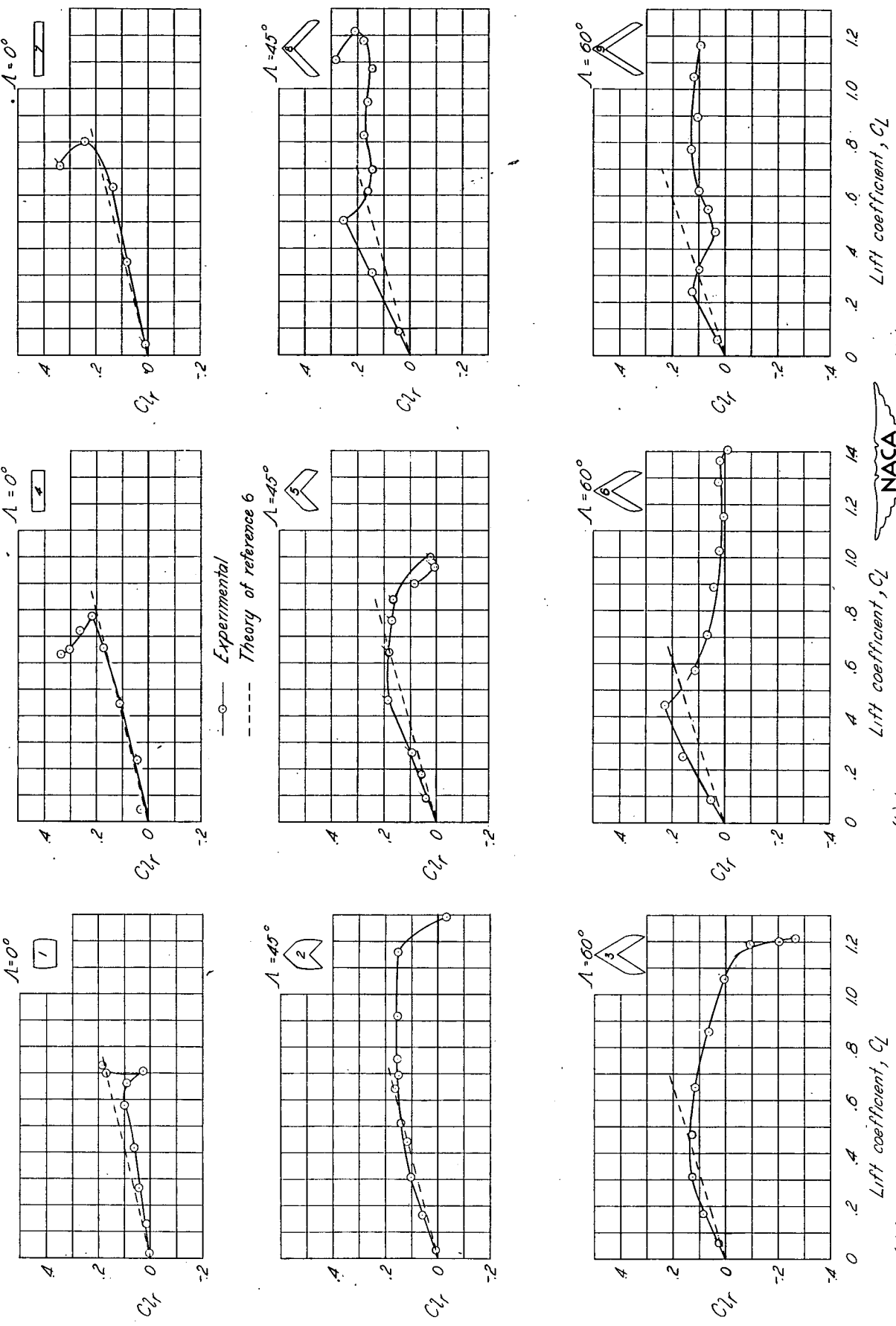
(F) $\Lambda = 60^\circ$, $A = 5.16$.
 Figure 10. - Concluded.





(a) $A = 1.34$.
 (b) $A = 2.61$.
 (c) $A = 5.16$.

Figure 11.- Variation of the experimental and theoretical values of C_{Nr} with lift coefficient for a series of swept wings.



(a) $A = 1.34$.
 (b) $A = 2.61$.
 (c) $A = 5.16$.
 Figure 12. - Variation of the experimental and theoretical values of C_L with lift coefficient for a series of swept wings.

A Experimental Theory of reference 6

1.34
2.61
5.16

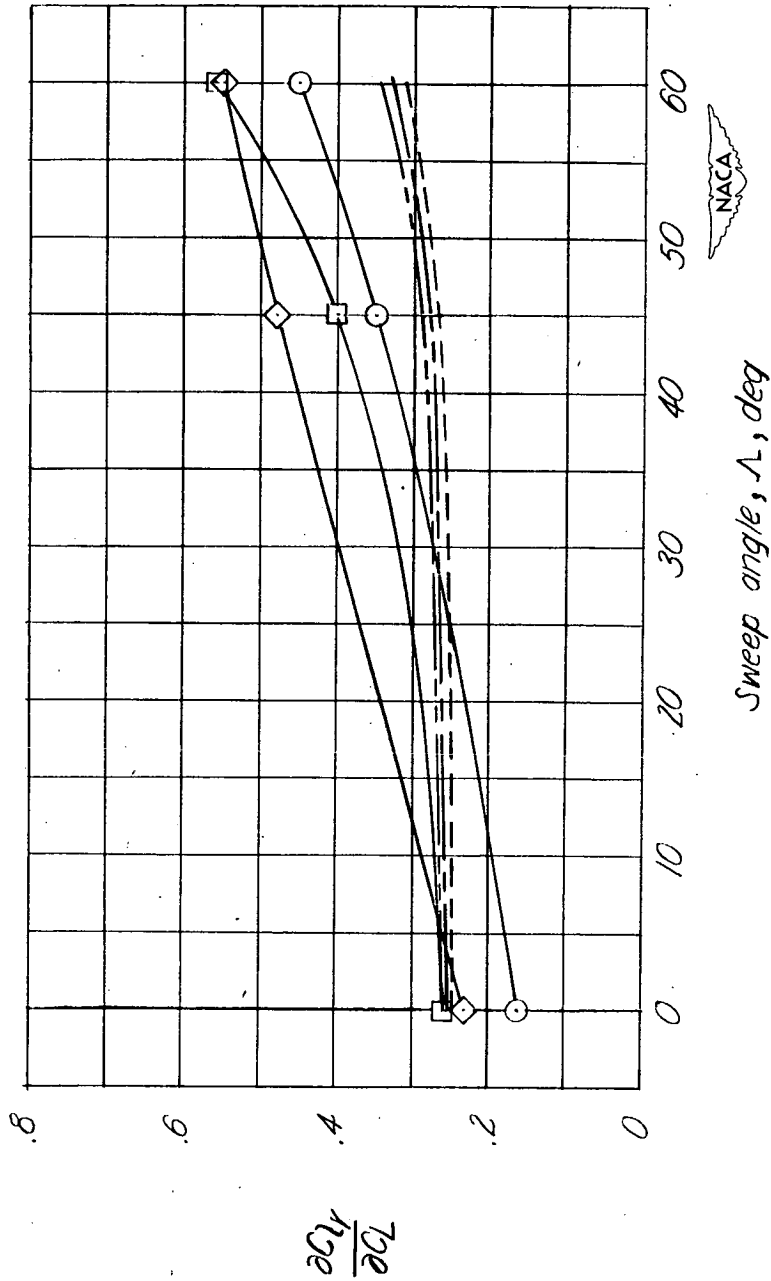


Figure 13.- Variation with sweep angle of the experimental and theoretical values of $\frac{\partial C_L}{\partial \alpha} / \frac{\partial C_L}{\partial \Lambda}$.

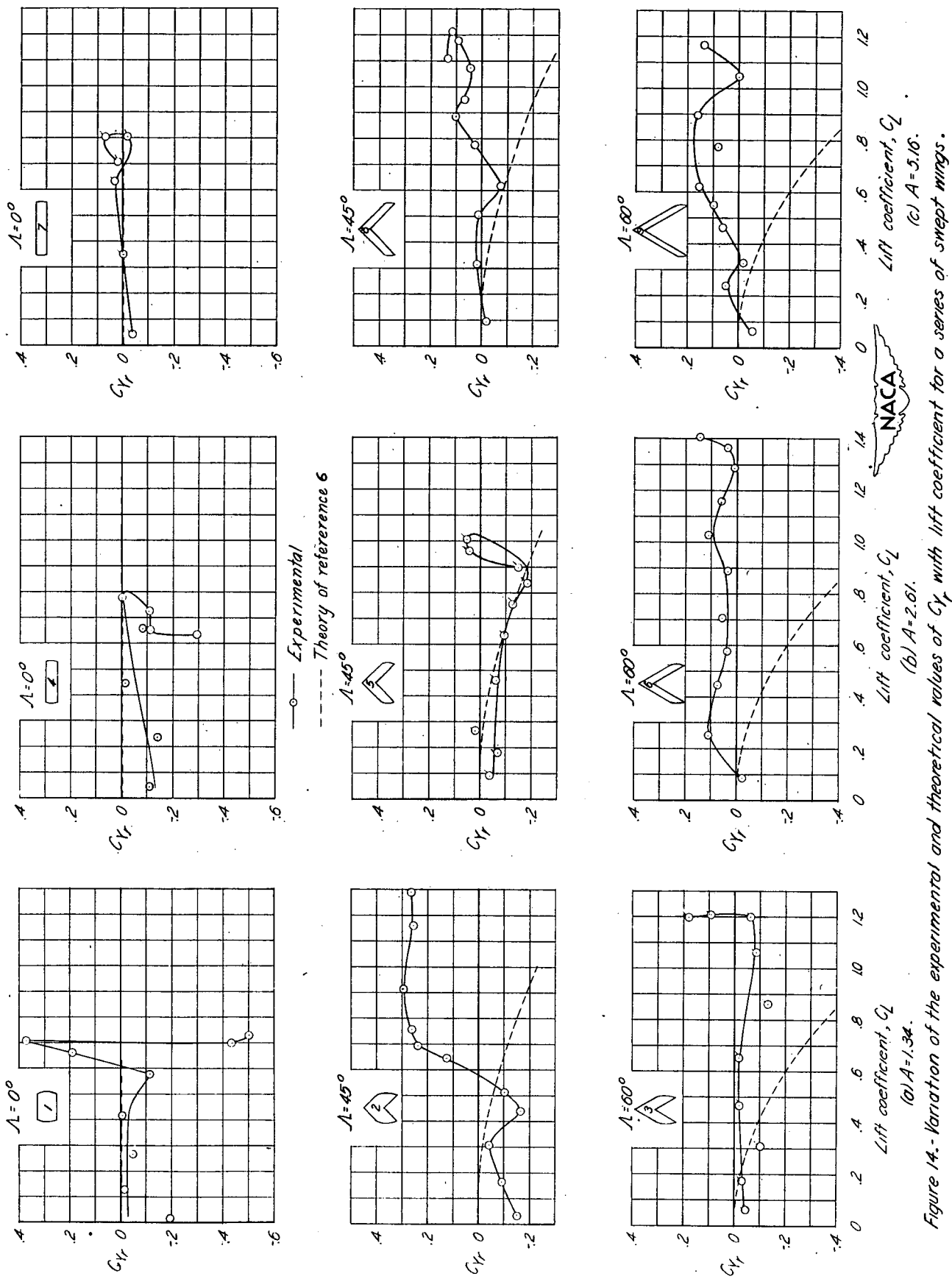


Figure 14.- Variation of the experimental and theoretical values of C_y with lift coefficient for a series of swept wings.
 (a) $A=1.34$.
 (b) $A=2.61$.
 (c) $A=5.16$.